Comprehensive Status Report: November 18, 2004

OTRC Project Title: Suction Caissons & Vertically Loaded Anchors
MMS Project 362 TO 16169
Project Subtitle: Suction Caissons: Finite Element Studies
PI: John L. Tassoulas
MMS COTR: A. Konczvald

This report provides a comprehensive summary of the research completed in all prior Phases of this project (September 1999 – August 2004), and describes research being done in the present Phase (September 2004 – August 2005) to complete this project.

Note that this report addresses one of four related research areas on this project. The other three areas are reported separately under the subtitles – Suction Caissons: Model Tests, Suction Caissons: Seafloor Characterization for Deepwater Foundation Systems, and Suction Caissons & Vertically Loaded Anchors: Design Analysis Methods.

Suction Caissons: Finite Element Modeling

John L. Tassoulas,[a] Dilip R. Maniar,[b] and L.F. Gonzalo Vásquez[c]

SUMMARY

This Report presents an overview of efforts at the Offshore Technology Research Center toward development and validation of a computational procedure suitable for simulations of suction caisson behavior under axial and lateral loads considering the effects of installation into clayey soil by self-weight and suction. The soil is a treated as a two-phase medium: a water-filled porous solid. Nonlinear behavior of the solid phase (soil skeleton) is described by means of a bounding-surface plasticity model. A frictional contact algorithm based on a slide-line formulation is used to analyze interaction between the caisson and the surrounding soil. The contact formulation allows large relative displacement between the caisson and the soil. In addition, a remeshing tool eliminates the need for a priori specification of the caisson penetration path: as installation of the caisson progresses, the finite-element mesh is adjusted so that the line of nodes below the caisson tip remains straight in the axial direction.

A brief account of the computational procedure along with simulations of caisson installation, reconsolidation of the soil-skeleton and caisson pullout is provided. The computational results are compared with measurements from laboratory tests also conducted at the Offshore Technology Research Center.

INTRODUCTION

A suction caisson is a hollow cylinder (or tube) capped at the top. It is allowed to penetrate the seafloor bottom sediments under its own weight, and then pushed to the required depth with differential pressure applied by pumping water out of the caisson interior. The use of suction caissons as foundations for deep-water offshore structures and anchors for

[a] Principal Investigator, OTRC, Department of Civil Engineering, The University of Texas, Austin, TX 78712
[b] Graduate Research Assistant, OTRC, currently with Stress Engineering, Inc., Houston, TX 77041
[c] Graduate Research Assistant, OTRC, currently with Ensoft, Inc., Austin, TX 78728

mooring lines has been increasing in the last decade. Suction caissons are an attractive option with regard to providing anchorage for floating structures in deep water as they offer a number of advantages in that environment. They are easier to install than impact driven piles and can be used in water depths well beyond where pile driving becomes infeasible. Suction caissons have higher load capacities than drag embedment anchors and can be inserted reliably at preselected locations and depths with minimum disturbance to the seafloor environment and adjacent facilities (Sparrevik 2001).

Better and reliable understanding of suction caisson behavior has been sought by means of field tests, laboratory tests, and numerical simulations. Extensive field tests on small-scale and full-scale caissons have been carried out to determine their installation characteristics and their axial and lateral load capacities, e.g. Hogervorst (1980), Tjelta et al. (1986), Tjelta (1995). Field tests are valuable in obtaining geotechnical information relevant in the design of future caissons, but they are expensive and time-consuming. On the other hand, laboratory testing of model suction caissons can be employed to investigate performance of the caissons under a variety of conditions. Geotechnical centrifuge tests on model suction caissons have been carried out to simulate the stress conditions and soil response at the field scale (see Clukey et al. 1995, Randolph et al. 1998). These are quite costly and remain subject to various limitations. Model suction caissons have been tested under 1-*g* and controlled laboratory conditions (Wang et al. 1977, Steensen-Bach 1992, Rao et al. 1997, El-Gharbawy and Olson 1999, El-Gharbawy et al. 1999, Whittle et al. 1998, Byrne and Houlsby 2002). The caissons studied were of aspect ratio (length-to-diameter ratio) in the range of 2-12 and were tested under various loading conditions. Laboratory tests on model suction caissons conducted by Wang et al. (1977) were focused on studying caisson efficiency and feasibility and identifying important parameters governing their performance. The recent laboratory tests (Rao et al. 1997, El-Gharbawy and Olson 1999) were focused on improving the design methodology.

Studies of suction caisson behavior involving extensive axisymmetric and three-dimensional numerical simulations (Sukumaran et al. 1999, Erbrich and Tjelta 1999, El-Gharbawy and Olson 2000, Deng and Carter 2002) have been carried out to determine their capacity under different loading and drainage conditions. Sukumaran et al. (1999) and Erbrich and Tjelta (1999) used the commercial finite element code ABAQUS (www.hks.com), El-Gharbawy and Olson (2000) used the commercial finite element code PLAXIS (http://www.plaxis.nl) developed for geotechnical computations, and Deng and Carter (2002) used the finite element software AFENA developed at the Center for Geotechnical Research at the University of Sydney (http://www.civil.usyd.edu.au/cgr). In all cases, the stress-strain behavior of the soil skeleton was represented by means of plasticity models such as the modified cam-clay model. The suction caisson was wished in place, with no attempt to simulate the installation process. Perfect interface bonding was assumed between the caisson and the surrounding soil skeleton. The initial state of stress in the soil skeleton was typically estimated in terms of the submerged unit weight and the lateral earth pressure coefficient at rest (Deng and Carter 2002).

The computational procedure developed in the course of the study (Vásquez 2000, Maniar 2004) reported herein simulates suction caisson installation and estimates the axial and lateral capacities. An axisymmetric formulation was implemented in a computer code for analysis of installation and axial-pullout problems. On the other hand, a three-dimensional analysis formulation that utilizes the general-purpose finite-element analysis code ABAQUS (http://www.hks.com) but imports the state of the state of the soil-caisson system from axisymmetric installation computations was used in lateral-pullout analysis. The soil is

modeled with water-saturated porous solid finite elements and the caisson is discretized using (impermeable) solid finite elements. Nonlinear soil behavior is taken into account by means of a bounding-surface plasticity model. A frictional-contact algorithm based on a slide-line formulation is used in representing soil-caisson interface behavior. Various remeshing tools are developed to eliminate the need for a priori specification of the caisson penetration path and to avoid use of excessively distorted finite-elements along caisson-soil interfaces. Using the formulation developed, the numerical results are obtained from the simulation of the caisson installation and reconsolidation simulation of surrounding soil following caisson installation, and simulation of the caisson pullout. The computed caisson behavior is compared with measurements from laboratory tests conducted at The University of Texas at Austin (Mecham 2001, Luke 2002, Coffman 2003, Coffman et al. 2004).

GOVERNING EQUATIONS

The behavior of the saturated, porous, clayey soil is described using a mixture theory (Atkin and Craine 1976, Bowen 1976, Prevost 1980, 1981) that accounts for coupling between the soil-skeleton deformation and the pore-fluid motion. The saturated soil is thus modeled as a two-phase medium composed of solid (soil skeleton) and pore-fluid (water) phases.

Summarized below are the balance laws, governing the interaction or coupling between the soil-skeleton deformation and the pore-fluid motion, which are derived using mixture theory or Biot's theory (Biot 1941, 1955). The governing differential equations of the mixture are expressed in terms of solid displacements, Darcy's velocities, and the excess pore-fluid pressure.

Conservation of Mass

Assuming incompressibility and homogeneity of the soil particles that form the skeleton, the law of conservation of mass of the mixture can be expressed as:

$$div(\mathbf{V}^S) + div(\mathbf{V}^R) - \frac{n_w}{\lambda_w}\frac{\partial(p^w)}{\partial t} - \frac{n_w\gamma_w}{\lambda_w}[\mathbf{1}_z]^T\mathbf{V}^S - \frac{\gamma_w}{\lambda_w}[\mathbf{1}_z]^T\mathbf{V}^R - \frac{1}{\lambda_w}[grad(p^w)]^T\mathbf{V}^R = 0 \qquad (1)$$

where: $\mathbf{V}^S$ is the velocity of the solid phase, $\mathbf{V}^R$ is Darcy's velocity defined as the relative velocity of the fluid phase with respect to the solid phase multiplied by the porosity (n_w), p^w is the excess pore-fluid pressure, λ_w is the bulk modulus of the fluid, γ_w is the specific weight of the fluid, and $\mathbf{1}_z$ is the unit vector in the vertical direction. The *div* and *grad* are the spatial divergence and spatial gradient operators, respectively.

Conservation of Linear Momentum

The total Cauchy stress tensor $(\boldsymbol{\sigma})$, can be written as the sum of the *effective* stress tensor $(\boldsymbol{\sigma}^{eff})$ and the excess pore-fluid pressure as:

$$\boldsymbol{\sigma} = \boldsymbol{\sigma}^{eff} + p^w\mathbf{I} \qquad (2)$$

The conservation of linear momentum of the fluid phase can be written as:

$$-\rho_w \mathbf{a}^S - \frac{\rho_w}{n_w}\mathbf{a}^R + grad\left(p^w\right) - \frac{\rho_w}{n_w}\mathbf{k}^{-1}\mathbf{V}^R = \mathbf{0} \tag{3}$$

where: ρ_w is the mass density of the fluid phase, $\mathbf{a}^S$ is the acceleration of the solid phase, $\mathbf{a}^R$ is the relative acceleration between the fluid and solid phases, and $\mathbf{k}$ is the permeability matrix of the soil skeleton.

The conservation of linear momentum of the mixture can be written as:

$$\left[\rho_S(1-n_w) + \rho_w n_w\right]\left(\mathbf{b} - \mathbf{a}^S\right) + \rho_w\left(\mathbf{b} - \mathbf{a}^R\right) + div\left(\boldsymbol{\sigma}^{eff}\right) + grad\left(p^w\right) = \mathbf{0} \tag{4}$$

where: ρ_S is the mass density of the solid phase, and $\mathbf{b}$ is the body force per unit volume of the solid phase.

FINITE-ELEMENT DISCRETIZATION

The axisymmetric discretization of soil-skeleton is accomplished with eight-node, quadratic, isoparametric, underintegrated finite elements for solid displacements, and Darcy's velocities, with interpolation functions $\mathbf{N}_S$ and $\mathbf{N}_R$, respectively. Spatially continuous discretization of excess pore-fluid pressure is applied using four-node bilinear finite elements with interpolation functions $\mathbf{N}_P$.

The weak statements corresponding to the governing differential equations can be obtained following standard variational arguments. The tangent stiffness matrix required for Newton iterations can be derived using consistent linearization of the weak statements. Adopting finite element discretization and approximations for field variables (solid displacements, Darcy's velocities and excess pore-fluid pressure), following weak statements are obtained:

$$\begin{aligned}
&-\int_{\Gamma_q}\left(\mathbf{N}_P\right)^T q dA + \int_\Omega \left[grad\left(\mathbf{N}_P\right)\right]^T \mathbf{V}^R J dV - \int_\Omega \left(\mathbf{N}_P\right)^T div\left(\mathbf{V}^S\right) J dV \\
&+\int_\Omega \left(\mathbf{N}_P\right)^T \frac{n_w J}{\lambda_w}\frac{\partial\left(p^w\right)}{\partial t} dv + \int_\Omega \left(\mathbf{N}_P\right)^T \frac{J}{\lambda_w}\left[grad\left(p^w\right)\right]^T \mathbf{V}^R dV \\
&+\int_\Omega \left(\mathbf{N}_P\right)^T \frac{n_w \gamma_w J}{\lambda_w}\left(\mathbf{1}_z\right)^T \mathbf{V}^S dV + \int_\Omega \left(\mathbf{N}_P\right)^T \frac{n_w J}{\lambda_w}\left(\mathbf{1}_z\right)^T \mathbf{V}^R dV = 0
\end{aligned} \tag{5}$$

$$\begin{aligned}
&\int_{\Gamma_R}\left(\mathbf{N}_R\right)^T \mathbf{T}^w dA - \int_\Omega \left[div\left(\mathbf{N}_R\right)\right]^T \left(p^w\right) J dV - \int_\Omega \left(\mathbf{N}_R\right)^T \rho_w J \mathbf{a}^S dV \\
&-\int_\Omega \left(\mathbf{N}_R\right)^T \frac{\rho_w J}{n_w}\mathbf{a}^R dV - \int_\Omega \left(\mathbf{N}_R\right)^T \frac{\rho_w J}{n_w}\mathbf{k}^{-1}\mathbf{V}^R dV = \mathbf{0}
\end{aligned} \tag{6}$$

$$\int_{\Gamma_S} \left(\mathbf{N}_S\right)^T \mathbf{T}^{Tot} dA - \int_{\Omega} \left[grad\left(\mathbf{N}_S \delta \mathbf{U}_S\right)\right]^T \boldsymbol{\sigma}^{eff} J dV$$
$$- \int_{\Omega} \left[div\left(\mathbf{N}_S\right)\right]^T p^w J dV - \int_{\Omega} \left(\mathbf{N}_S\right)^T \left(\rho_S - \rho_w\right)\left(1 - n_0\right)\mathbf{b} dV \qquad (7)$$
$$- \int_{\Omega} \left(\mathbf{N}_S\right)^T \left[\rho_S\left(1 - n_0\right) + \rho_w n_w J\right]\mathbf{a}^R dV = \mathbf{0}$$

The first term in Eq. 7 is the virtual work of the surface traction due to total stresses, which, within the finite element framework, leads to the (consistent) definition of the equivalent total force. Similarly, the first term in Eq. 6 is the virtual work of the surface tractions due to excess pore-fluid pressure, giving rise to the equivalent excess pore-fluid force. Therefore, the virtual work of the surface tractions due to effective stresses, or the equivalent effective force, can be obtained as the difference between the former and the later. This way of extracting the forces due to effective traction is possible because of the way the governing equations are crafted and the fact that the interpolation functions adopted for the solid displacements and Darcy's velocities are identical. The contact formulation described below makes use of this fact in order to estimate the equivalent frictional force as a function of the equivalent effective normal force.

The caisson is represented using conventional, axisymmetric, solid finite elements: eight-node, quadratic, isoparametric elements for displacements.

SOIL CONSTITUTIVE MODEL

The nonlinear behavior of the clayey soil is modeled through a bounding-surface plasticity model for isotropic cohesive soils (Dafalias and Herrmann 1982, Dafalias 1986, Dafalias and Herrmann 1986, Kaliakin and Herrmann 1991). The model is based on the concepts and principles of critical state soil mechanics. The bounding surface is a reliable and versatile concept for representation of clay behavior along arbitrary stress and strain paths. The constitutive model provides the relationship between soil effective stress and strain increments.

SOIL-CAISSON INTERFACES

The interior and exterior soil-caisson interfaces are modeled with a contact algorithm based on a slide-line formulation (Hallquist et al. 1985), which allows for large relative displacements between the caisson and the soil. The slide-line formulation involves nodes on the soil side of the interface and surface elements on the caisson side.

In the contact algorithm, penetration of soil nodes into the caisson is prevented with constraints imposed on the solid displacement, Darcy's velocity, and the excess pore-fluid pressure using Lagrange multipliers. Friction between the soil and the caisson is assumed to obey the classical Coulomb law. "Stick" and "slip" conditions are distinguished on the basis of the level of interface frictional force in comparison with the Coulomb force, which is taken equal to the effective compressive (normal) force multiplied by the soil-caisson interface friction coefficient. Therefore, for a slave node that is in contact with a surface element, contact contributions arising from constraining solid displacement, Darcy's velocity, and excess pore-fluid pressure and contribution from the frictional interface must be added in the tangent stiffness matrix during Newton iterations.

The slide-line contact formulation is developed in terms of effective forces along the interface, which are integrals of the effective traction along the interface. By the arrangement of the governing differential equations and the corresponding weak statements, it is straightforward to extract these effective forces along the interface.

POTENTIAL FLOW

During installation of the caisson, by self-weight or suction, water flows out of the caisson interior through holes in the top cap. The size of the holes is considerably smaller than the interior cross section of the caisson. Therefore, water cannot flow freely and some change in pressure is expected in the interior of the caisson. To simulate this phenomenon, a potential flow formulation was used to estimate the pressure generated at the top of the interior soil during various stages of the simulation (Vásquez 2000). The potential flow formulation is developed on the basis of assumptions that the fluid is incompressible and inviscid and its flow is irrotational.

REMESHING

A remeshing tool was developed to eliminate the need for a priori specification of the caisson penetration path. As installation of the caisson progresses, the finite-element mesh is adjusted so that the line of nodes below the tip remains straight in the axial direction. By performing this adjustment, it is possible to eliminate overconfinement of the soil in the caisson interior, thus permitting calculation of the path of penetration in the soil domain (Maniar and Tassoulas 2002, Maniar 2004).

Another remeshing tool was developed to adjust the finite-element mesh along the caisson-soil interfaces. This tool is intended for eliminating distortion of the soil elements along the caisson-soil interfaces and is convenient in cases where a high coefficient of friction on the soil-caisson interfaces leads to significant finite-element distortion. This second remeshing tool was not used in the simulations described below, as it turned out to be unnecessary for this case.

Mapping of field variables from the current finite-element mesh to the adjusted one is carried out using least squares estimation (Hinton and Campbell 1974), also referred to as global smoothening procedure, applied over the selected set of finite-elements along and below the caisson. Quadratic interpolation functions are adopted for mapping of field variables.

SIMULATION PROCEDURE

Typical computations are carried out in a sequence that closely follows both laboratory and field tests. The sequence of steps is: a) preparation of the soil test bed starting with the original slurry, b) installation of the caisson; self-weight and suction, c) reconsolidation of the soil; and d) pullout of the caisson under either drained or undrained conditions. For the first step, the initial state of the soil domain is obtained from the experimental data. For each of the remaining steps, the initial state of the soil domain is obtained from the end of the previous step.

SIMULATION RESULTS AND VERIFICATION

The computational formulation outlined above is applied to the analysis of model suction caissons installed and tested at The University of Texas at Austin (Luke 2002, Coffman 2003). In this section, the computational results are presented and verified by comparison with the experimental data.

Preparation of Soil Test bed

The soil test bed was formed by allowing slurry of kaolinite to consolidate under self-weight, resulting in normally consolidated clay. Details of the preparation and consolidation of the test bed are presented elsewhere (Pedersen 2001, Olson et al. 2003). The consolidation of kaolinite slurry was simulated by analyzing a 24-in diameter kaolinite slurry cylinder with 61-in initial height (same as in the test) and frictional contact on the lateral impermeable surface (container wall). The time required for consolidation was found to be about 6 months, close to the seven-month period recorded in the laboratory, and the computed final slurry height at the axis of the soil cylinder was 44.6 in, close to a measurement of 43.4 in taken at about the same distance from the wall of the steel tank in which the test bed was prepared (Fig. 1). It is worth mentioning that the three-dimensional (axisymmetric) soil state obtained at the end of the initial-consolidation simulation is critical to success in later computations of caisson response during installation and pullout because of the noticeably weaker soil obtained as a result of friction on the container wall (Maniar 2004). The more straightforward one-dimensional consolidation simulation overestimates the soil strength in the vicinity of the axis by about 30% (Maniar 2004).

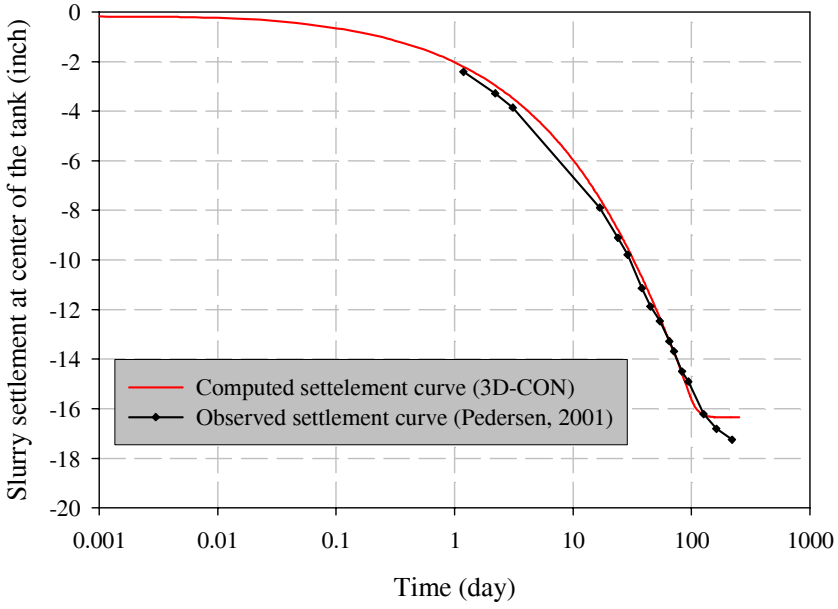

Figure 1: Observed and computed consolidation curves for the kaolinite slurry.

Self-Weight Installation

In one of the modes of installation examined in the laboratory, the 4-in exterior-diameter model caisson penetrated 32 in under self-weight in about 200 sec. The simulation of self-weight installation was conducted in a similar manner. The computed and measured excess

pore-water pressures, recorded at five locations, on interior and exterior wall surfaces of the model caisson during self-weight installation are plotted versus the position of the caisson tip in Fig. 2. Good agreement can be seen, especially at interior locations away from the caisson tip. The so-called "penetration path" (Maniar 2004), i.e., the undeformed surface (line in axisymmetric geometry) on which penetration occurs is shown in Fig. 3. It can be seen that, in the self-weight mode of installation, soil is displaced outwards.

Suction Installation

In the other mode of installation considered in the laboratory tests, the 4-in exterior-diameter model caisson penetrated 16 in under self-weight in about 69 sec and, subsequently, suction was applied resulting in additional 16 in penetration in about 420 sec. The simulation of this self-weight-followed-by-suction installation, referred to as suction installation below for simplicity) was conducted in a similar manner. The computed and measured excess pore-fluid pressures are in very good at all interior locations and the exterior location away from the tip (O1) but substantial difference was found at the exterior location next to the tip (Maniar 2004). The plot of cumulative soil displaced during penetration shows (Maniar 2004) that, in this mode of installation, a small amount of soil is displaced outwards during the self-weight installation segment but, as expected, soil is drawn into the caisson interior during the suction segment.

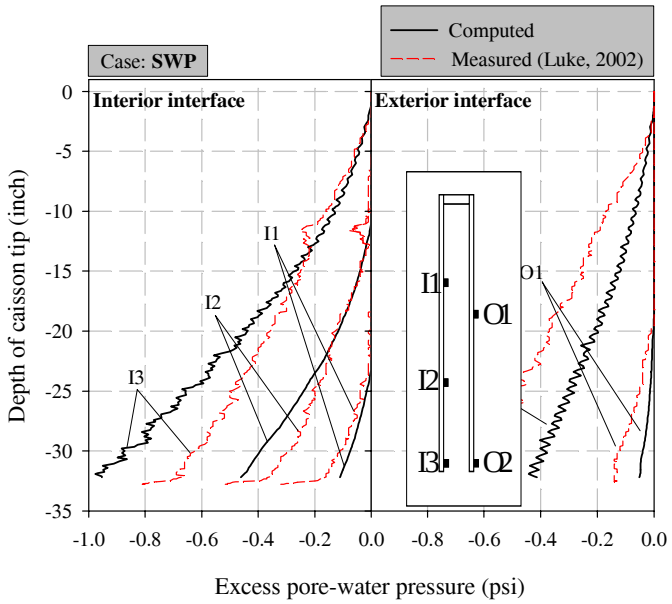

Figure 2: Pore-water pressure: computations and measurements during self-weight caisson installation.

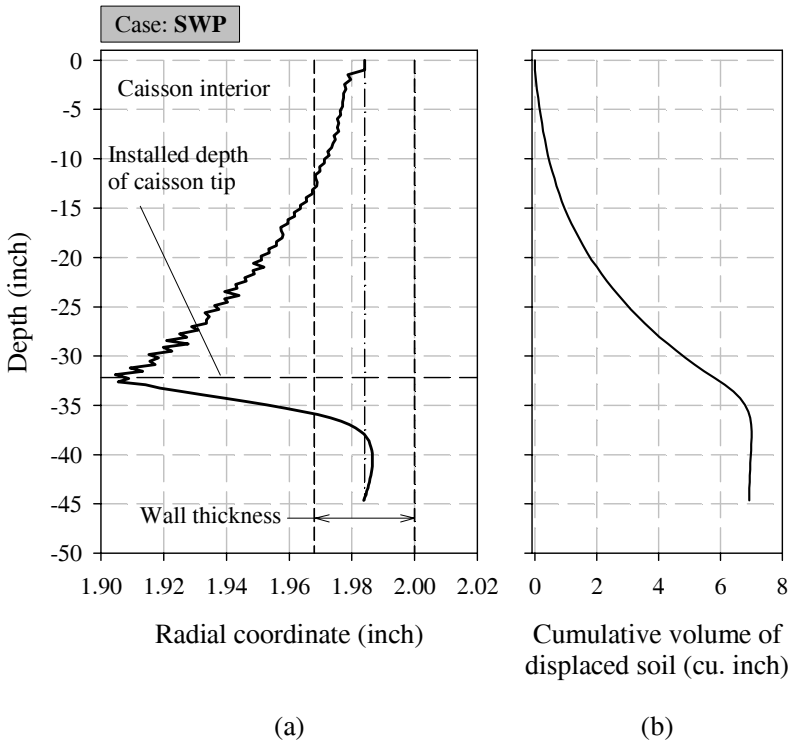

Figure 3: Self-weight penetration path (a) and cumulative volume of displaced soil (b).

Reconsolidation

In both the tests (Coffman 2003) and the simulations, the excess pore-water pressures generated during caisson installation were reduced to negligible levels after about 96 hours of reconsolidation. The computed and measured pore-water pressure time histories are in good agreement as well (Maniar 2004). Fig. 4 depicts the distribution of radial stress after reconsolidation for the case of suction installation. It can be seen that the level of radial stress in the interior of the caisson is higher than in the exterior, especially in the vicinity of the tip. Furthermore, at a depth of about 16 in, where the installation mode was switched from self-weight to suction, there is notably higher radial stress in the caisson exterior, apparently resulting from soil having been “pushed” outwards.

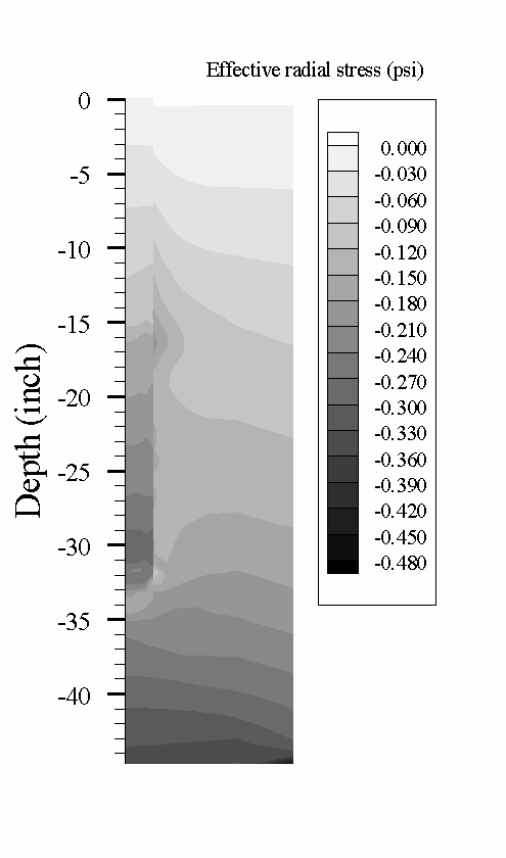

Figure 4: Radial stress distribution after reconsolidation following suction installation.

Axial Pullout

Starting from each of the two installations, by self-weight penetration (SWP) and suction (SUC), described above, axial-pullout simulations were conducted under a variety of conditions: vented (V) or closed (C) cap, rapid (R), slow (S), or drained (D) pullout (for explanation of these conditions, see Maniar 2004). Not all combinations of installations and conditions have been tested in the laboratory. Table 1 summarizes the computational results regarding axial capacity and the available experimental data along with the computed contributions to resistance from interior friction, exterior friction and suction. The agreement between computations and measurements is good with maximum difference of about 20%. It is worth noting that both the simulations and the experiments indicate clearly that the capacity of suction caissons installed by self-weight penetration is higher than by suction installation, regardless of pullout speed and independently of whether the cap is vented or closed. The increase in capacity of caissons installed by self-weight appears to be related to the higher soil strength reached in this mode of installation (Maniar 2004).

Table 1: Computed and measured axial capacities (see Section on Axial Pullout for explanation of symbols).

Simulation	Measured Capacity (Luke, 2002) (lb)	Computed capacity (lb)	Exterior friction (%)	Interior friction (%)	Total friction (%)	Suction force (%)
SWP-VR	24.0	20.4	52.2	37.4	89.6	-
SWP-VS	-	17.8	58.7	29.4	88.1	-
SWP-VD	-	18.5	53.8	34.8	88.6	-
SWP-CR	28.0	23.4	42.1	7.0	49.1	41.9
SUC-VR	19.2	18.2	40.1	48.3	88.4	-
SUC-VS	-	14.8	48.1	37.6	85.7	-
SUC-VD	20.0	17.3	41.9	45.8	87.7	-
SUC-CR	18.6	22.7	32.2	14.2	46.4	44.3

Lateral Pullout

Abaqus (http://www.hks.com) was used for three-dimensional simulations of caissons subjected to lateral loads, horizontal, or, in general, inclined loads. The soil stresses and state parameters as computed from the installation analysis (self-weight or suction) conducted using the axisymmetric finite-element code developed in the course of this study were imported into Abaqus as initial conditions and, subsequently, the lateral-pullout computations were carried out (see Maniar 2004) for further details. Shown in Fig. 5 (a) are the computed and measured horizontal capacities, in the case of suction installation, considering different locations of the point of load application (pad eye). The agreement is excellent. Both the computations and the measurements indicate that the horizontal capacity is highest for a pad eye located at about 2/3 of the installation depth. Self-weight installation leads to a small increase in horizontal capacity, as can be seen in Fig. 5 (b).

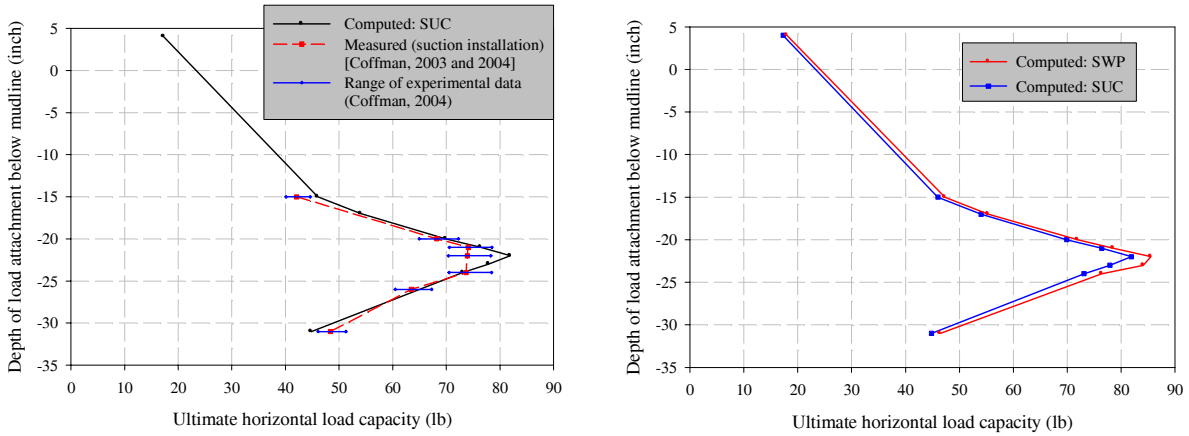

Figure 5: Horizontal capacity: (a) computations and measurements, (b) effect of installation mode.

The interaction diagram provided in Fig. 6 shows the capacities computed for inclined loads applied at about the optimal (2/3-point) pad-eye location.

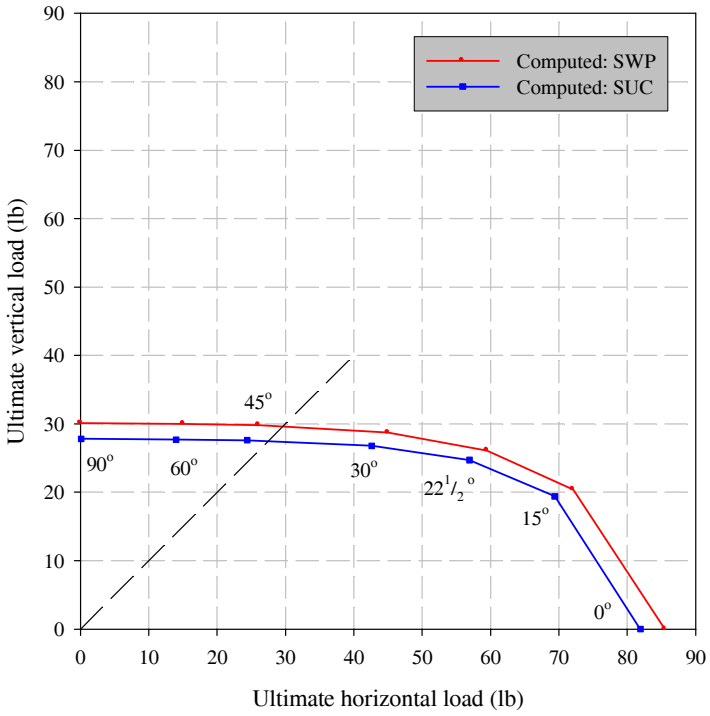

Figure 6: Interaction diagram for inclined loads applied at the optimal pad-eye location

The deformed configuration of the soil-caisson system, following installation by suction, and the distribution of radial effective stress, in the plane defined by the caisson axis and the applied horizontal force, are shown in Fig. 7 for the peak level of load acting at the optimal pad-eye location. It is clear that the caisson undergoes very little, hardly noticeable rotation prior to pullout under this optimal horizontal force.

CONCLUSIONS

A computational procedure has been developed at the Offshore Technology Research Center for the analysis of suction caisson behavior under both axial and lateral loads. The procedure has been used in simulations of tests conducted in the course of a concurrent OTRC project at The University of Texas at Austin on caisson models. Computational results and experimental data regarding all facets of the tests have been found to be in good agreement. Installation by self-weight and suction, soil reconsolidation, and axial, horizontal and inclined pullout have been examined.

Further work, currently underway, involves simulations of centrifuge tests of suction caissons and additional 1-g tests on caisson models as well as documentation of the finite-element code that has been developed.

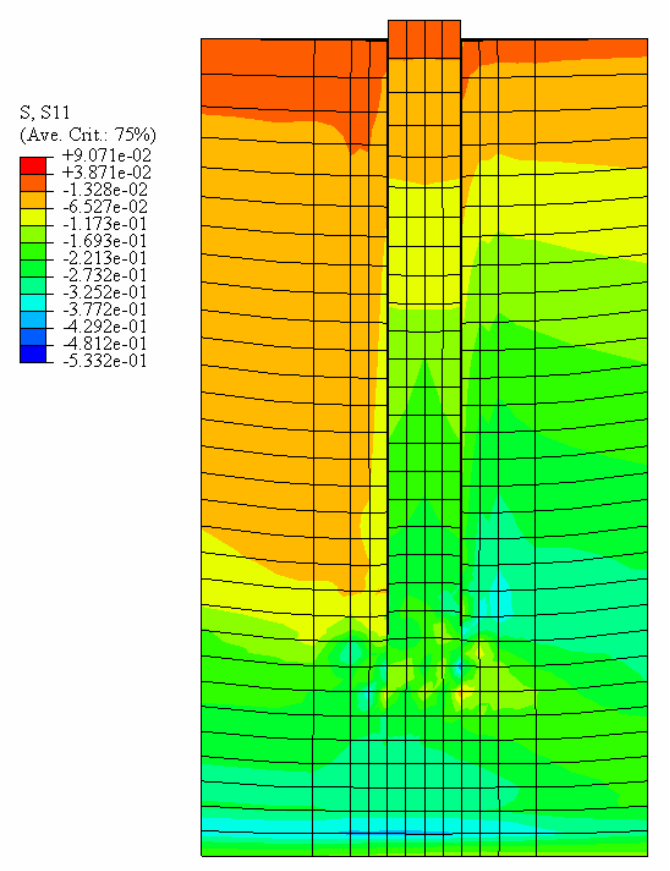

Figure 7: Radial effective stress distribution at maximum horizontal capacity.

REFERENCES

Atkin, R.J., and Craine, R.E. 1976. "Continuum theories of mixtures: Basic theory and historical development," Quarterly Journal of Mechanics and Applied Mathematics, Vol. 29, pp. 209-244.

Biot, M.A. 1941. "General theory of three dimensional consolidation," Journal of Applied Physics, Vol. 12, pp. 155-164.

Biot, M.A. 1955. "Theory of elasticity and consolidation of porous anisotropic solid," Journal of Applied Physics, Vol. 26, pp. 182-185.

Bowen, R.M. 1976. "Theory of mixtures," Continuum physics, Ed. A.C. Eringen, Academic Press, New York, pp. 1-127.

Byrne, B.W., and Houlsby, G.T. 2002. "Experimental investigations of response of suction caissons to transient vertical loading," Journal of Geotechnical and Geoenvironmental Engineering, Vol. 128, No. 11, pp. 926-939.

Clukey, E. C., Morrison, M. J., Gariner, J., and Corté, J. F. 1995. "The response of suction caissons in normally consolidated clays to cyclic TLP loading conditions," Proceedings, Offshore Technology Conference, OTC 7796, pp. 909-918.

Coffman, R.A. 2003. "Horizontal capacity of suction caissons in normally consolidated kaolinite," M.S. Thesis, The University of Texas at Austin.

Coffman, R.A., El-Sherbiny, R.M., Rauch, A.F., and Olson, R.E. 2004. "Measured horizontal capacity of suction caissons," OTC 16161, Proceedings, Offshore Technology Conference, Houston, Texas.

Dafalias, Y.F., and Hermann, L.R. 1982. "Bounding surface formulation in soil plasticity," Chapter 10 in Soil mechanics – Transient and cyclic loads, Ed., G.N. Pande and O.C. Zienkiewicz, John Wiley & Sons Ltd., New York.

Dafalias, Y.F. 1986. "Bounding surface plasticity I: Mathematical foundation and hypoplasticity," Journal of Engineering Mechanics, ASCE, Vol. 112, No. 9, pp. 966-987.

Dafalias, Y.F., and Herrmann, L. R., 1986. "Bounding surface plasticity II: Application to isotropic cohesive soils," Journal of Engineering Mechanics, ASCE, Vol. 112, No. 12, pp. 1263-1291.

Deng, W., and Carter, J.P. 2002. "A theoretical study of the vertical uplift capacity of suction caissons," International Journal of Offshore and Polar Engineering, Vol. 12, No. 2, pp. 89-97.

El-Gharbawy, S., and Olson, R. 1999. "Suction caisson foundations in the Gulf of Mexico," Analysis, Design, Construction, and Testing of Deep Foundations, ASCE Geotech. Special Pub. 88, pp. 281-295.

El-Gharbawy, S.L., and Olson, R.E. 2000. "Modeling of suction caisson foundations," Proceedings of the International Offshore and Polar Engineering Conference, Vol. 2, pp. 670-677.

El-Gharbawy, S.L., Olson, R.E., and Scott, S.A. 1999. "Suction anchor installations for deep Gulf of Mexico applications," Proceedings, Offshore Technology Conference, OTC 10992, pp. 747-754.

Erbrich, C.T., and Tjelta, T.I. 1999. "Installation of bucket foundations and suction caissons in sand – Geotechnical performance," Proceedings, Offshore Technology Conference, OTC 10990, pp. 725-735.

Hallquist, J.O., Goudreau, G.L., and Benson, D.J. 1985. "Sliding interfaces with contact-impact in large-scale Lagrangian computations," Computer Methods in Applied Mechanics and Engineering, Vol. 51, pp. 107-137.

Hinton, E., and Campbell, J.S. 1974. "Local and global smoothening of discontinuous finite element functions using a least squares method," International Journal for Numerical Methods in Engineering, Vol. 8, pp. 461-480.

Hogervorst, J. R. 1980. "Field trials with large diameter suction piles," Proceedings, Offshore Technology Conference, OTC 3817, pp. 217-224.

Kaliakin, V. N., and Herrmann, L. R. 1991. "Guidelines for implementing the elastoplastic-viscoplastic bounding surface model," Technical Report, Department of Civil Engineering, University of California, Davis.

Luke, A. M. 2002. "Axial capacity of suction caisson in normally consolidated kaolinite," M.S. Thesis, The University of Texas at Austin.

Maniar, D.R. 2004. "A computational procedure for simulation of suction caisson behavior under axial and inclined loads," Ph.D. Dissertation, The University of Texas at Austin, 2000.

Maniar, D. R., and Tassoulas, J. L. 2002. “Nonlinear finite element simulation of suction caisson behavior,” Proceedings, Fifteenth ASCE Engineering Mechanics Conference, New York, New York.

Meacham, E.C. 2001. “A laboratory for measuring the axial and lateral capacity of model suction caisssons,” M.S. Thesis, The University of Texas at Austin.

Olson, R. E., Rauch, A. F., Mecham, E. C., and Luke, A. M. 2003. “Self-weight consolidation of large laboratory deposits of clay,” Proc., 12th Pan-American Conf. on Soil Mechanics and Geotechnical Engineering, Cambridge, Massachusetts.

Pedersen, R.C. 2001. “Model offshore soil deposit: design, preparation and characterization,” M.S. Thesis, The University of Texas at Austin.

Prevost, J.H. 1980. “Mechanics of continuous porous media,” International Journal of Engineering Science, Vol. 18, pp. 787-800.

Prevost, J.H. 1981. “Consolidation of anelastic porous media,” Journal of Engineering Mechanics Division, ASCE 107, EM1, pp 169-186.

Randolph, M. F., O’Neill, M. P., and Stewart, D. P. 1998. “Performance of suction anchors in fine-grained calcareous soils,” Proceedings, Offshore Technology Conference, OTC 8831, pp. 521-529.

Rao, S. N, Ravi, R., and Ganapathy, C. 1977. “Pullout behavior of model suction anchors in soft marine clays,” Proceedings, Seventh International Offshore and Polar Engineering Conference, Honolulu.

Sparrevik, P. 2001. “Suction pile technology and installation in deep waters,” Proceedings, OTRC 2001 International Conference, Geotechnical, Geological, and Geophysical Properties of Deepwater Sediments, Houston, pp. 182-197.

Steensen-Bach, J. O. 1992. “Recent model tests with suction piles in clay and sand,” Proceedings, Offshore Technology Conference, OTC 6844, pp. 323-330.

Sukumaran, B., McCarron, W.O., Jeanjean, P., and Abouseeda, H. 1999. “Efficient finite element techniques for limit analysis of suction caissons under lateral loads,” Computers and Geotechnics, Vol. 24, pp. 89-107.

Tjelta, T. I. 1995. “Geotechnical experience from the installation of the Europipe jacket with bucket foundations,” Proceedings, Offshore Technology Conference, OTC 7795, pp. 897-908.

Tjelta, T. I., Guttormsen, T. R., and Hermstad, J. 1986. “Large-scale penetration test at a deepwater site,” Proceedings, Offshore Technology Conference, OTC 5103, pp. 201-212.

Vásquez, L.F.G. 2000. “Computational procedure for the estimation of pile capacity including simulation of the installation process,” Ph.D. Dissertation, The University of Texas at Austin.

Wang, M. C., Demares, K. R., and Nacci, V. A. 1977. “Application of suction anchors in the offshore technology,” Proceedings, Offshore Technology Conference, OTC 3203, pp. 1311-1320.

Whittle, A. J., Germaine, J. T., and Cauble, D. F. 1998. “Behavior of miniature suction caissons in clay,” Offshore Site Investigation and Foundation Behaviour ’98, SUT, pp. 279-300.